analytical chemistry

Article

pubs.acs.org/ac

One-Pot Synthesis of Aptamer-Functionalized Silver Nanoclusters for Cell-Type-Specific Imaging

Jingjing Li, Xiaoqin Zhong, Fangfang Cheng, Jian-Rong Zhang, Li-Ping Jiang,* and Jun-Jie Zhu*

State Lab of Analytical Chemistry for Life Science (MOE), School of Chemistry and Chemical Engineering, Nanjing University, Nanjing 210093, People's Republic of China

Supporting Information

ABSTRACT: As an emerging category of fluorescent metal nanoclusters, oligonucleotide-templated silver nanoclusters (Ag NCs) have attracted a lot of interest and have shown wide application in biorelated disciplines. However, the weak fluorescence emission and poor permeability to cell membranes tethered further intracellular applications of Ag NCs. AS1411 is an antiproliferative G-rich phosphodiester oligonucleotide and currently an anticancer agent under phase II clinical trials. Herein, we present a strategy to synthesize AS1411-functionalized Ag NCs with excellent fluorescence through a facile one-pot process. Confocal laser scanning microscopy and *Z*-axis scanning confirmed that the AS1411-functionalized Ag NCs could be internalized into MCF-7 human breast cancer cells and were able to specifically stain nuclei with red color. To our surprise, 3-[4,5-dimethylthiazol-z-yl]-2,5-diphenyltetrazolium bromide (MTT) assay demonstrated the Ag NCs were cytocompatible and showed better inhibition effects than pure AS1411 on MCF-7 human breast cancer cells. In addition, a universal design of the oligonucleotide scaffold for synthesis of Ag NCs was extended to other aptamers, such as Sgc8c and mucin 1 aptamer. Due to the facile synthesis procedure and capability of specific target recognition, this fluorescent platform will potentially broaden the applications of Ag NCs in biosensing and biological imaging.

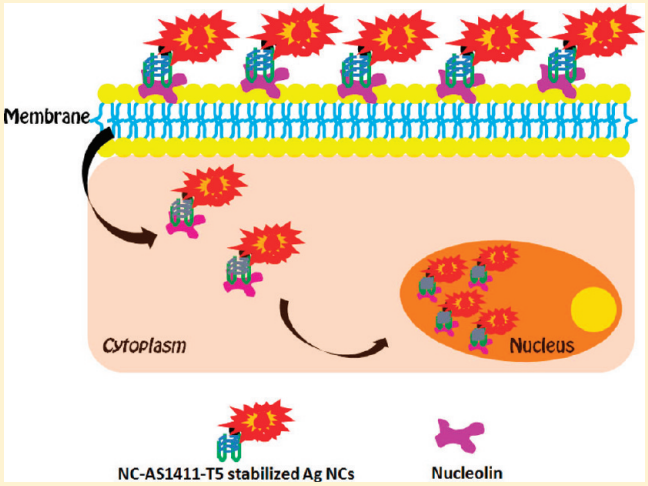

With the development of fluorescence microscope techniques and nanotechnology, fluorescence imaging has become one of the most powerful tools for the study of cellular processes, from studying early mammalian development at a cellular level to visualizing tumorigenesis in living animals.[1−3] Various functionalized quantum dots have been used as tools in imaging cellular structures and events.[4−8] Compared with organic dyes, quantum dots feature stronger fluorescent intensity and extraordinary photostability.[9,10] However, the relatively large physical size, strong fluorescence intermittency on all time scales, and constituent toxic elements compromise their widespread application.[11−13]

Recent advances in fluorescent metal nanoclusters, especially gold and silver, have attracted a lot of interest in biosensing and bionanotechnology.[14,15] It was reported that nanoclusters had excellent photostability, subnanometer size, and low toxicity, which complement the properties of organic dyes and semiconductor quantum dots.[16,17] Particularly, oligonucleotide-templated silver nanoclusters (Ag NCs) have attracted special attention due to their facile synthesis, tunable fluorescence emission, and high photostability.[18−20] The fluorescence emission of these DNA-stabilized silver nanoclusters can be tuned throughout the visible and near-IR range simply by modulating the sequence and length of oligonucleotides. DNA/Ag NCs have been successfully applied to discriminate a typical single-nucleotide mutation by taking advantage of their high dependence on the sequence of DNA scaffold.[21] Many other applications of DNA/Ag NCs in chemical and biological detection have also been reported. Chang and co-workers[22] developed a homogeneous fluorescence assay to detect Cu^{2+} by combining 3-mercaptopropionic acid (MPA) and DNA/Cu−Ag NCs in aqueous solution. Based on the fluorescence quenching of DNA/Ag NCs, the biothiols in the biological fluids were detected by Han and Wang.[23] Other applications included the detection of microRNA,[24] single-stranded DNA (ssDNA),[25,26] thiol compounds,[27] Hg^{2+},[28] and Cu^{2+}.[29] In another assay developed in 2008, cytosine-12-protected silver nanoclusters were covalently conjugated with avidin or primary antibody and used for cell surface labeling.[30] The major issue of such design is that the natural activity of biomolecules modified on C12 oligo might be harmfully affected during the reduction of Ag NCs by either a chemical reduction agent or an irradiation source.[31] In 2009, this group

Received: February 3, 2012
Accepted: April 7, 2012
Published: April 7, 2012

   dx.doi.org/10.1021/ac3003402 | *Anal. Chem.* 2012, 84, 4140−4146

successfully transferred poly(acrylic acid)-stabilized Ag NCs to anti-actin Ab/C12 and anti-α-tubulin/C12 conjugates and obtained fluorogenic silver cluster biolabels for cell surface labeling.[32] Recently, an Ag cluster was synthesized with modified Sgc8c aptamer and specifically marked the nucleus of live cells.[33] All of these showed great promise of silver nanoclusters in biosensing and nanotechnology.

The nucleus is a membrane-enclosed organelle in eukaryotic cells. It maintains the integrity of genes and controls the activities of the cell by regulating gene expression. Various questions on trafficking, homing tumor targeting, and other nucleus-related events could be potentially be answered by nuclear imaging.[34] Unlike conventional harsh silver nanoparticle-based staining, Yu et al.[35] developed a mild staining method. They prepared peptide-encapsulated fluorescent silver nanoclusters based on a silver binding protein for the nuclear staining. However, the fluorescence quantum yield of nanoclusters was relatively low (~3%). Herein, we report AS1411-stabilized silver nanoclusters with high fluorescence quantum yield (~40.1%) for nuclear staining. A general approach to design aptamer-containing DNA oligos as the scaffold for the synthesis of aptamer-functionalized silver nanoclusters with outstanding fluorescence properties was also proposed. Improvement of the fluorescence quantum yield could minimize the dosage of fluorescence probes, reducing the cost and the risk for negative effects.

AS1411 is an antiproliferative G-rich phosphodiester oligonucleotide and currently an anticancer agent under phase II clinical trials. Its function as an aptamer to nucleolin has led to the identification of nucleolin as a new molecular target for cancer therapy.[36,37] In this study, we rationally connected AS1411 with poly(cytosine) via a -TTTTT- loop (called a T5 loop) and employed it as the scaffold to synthesize Ag NCs through a one-step process. The obtained Ag NCs emitted red color and the fluorescence quantum yield could reach 40.1%, which was beneficial to the applications of biological imaging. AS1411 retained its anticancer nature within the complex, and unexpectedly, functionalized Ag NCs demonstrated enhanced efficiency of growth inhibition compared with naked AS1411. In addition, such functionalized Ag NCs could be internalized into the cells and stain the nucleus via receptor-mediated endocytosis. It could improve the permeability of DNA protection groups for live cell imaging and help understand the therapeutic mechanism of AS1411.[38,39] We also hypothesized that the T5 loop is crucial to the fluorescence of Ag NCs. As a proof of concept, Sgc8c and mucin 1 (MUC 1) aptamer were chosen as the model aptamers. Sgc8c is a well-studied ssDNA aptamer that can specifically bind to acute lymphoblastic leukemia.[40,41] Mucin protein (MUC1) is a tumor marker in epithelial malignancies and was widely used in immunotherapeutics and diagnostics.[42] Sgc8c and MUC1 aptamer were linked to poly(cytosine) via T5 loop, similar to the design of AS1411. Synthesized Ag NCs exhibited a red color emission with fluorescence quantum yields of 48.0% and 25.2%, respectively. This specific fluorescence platform of Ag NCs will have more potential applications in biological areas.

EXPERIMENTAL SECTION

Chemicals and Materials. Silver nitrate (99+%), sodium borohydride, $NaBH_4$ (powder, 98%), disodium hydrogen phosphate, sodium dihydrogen phosphate, sodium chloride, trisodium citrate, citric acid, acetate, sodium acetate, tris(hydroxymethyl) aminomethane (Tris), ammonium acetate, paraformaldehyde, and glycerol were all purchased from Nanjing Chemical Reagents Factory (Nanjing, China). 4′,6-Diamidino-2-phenylindole (DAPI) and cell cultures were purchased from Nanjing KenGen Biotech Co. Ltd. (Nanjing, China). All oligos were synthesized and purified by Shanghai Sangon Biotechnology Co. Ltd. (Shanghai, China) and sequences are listed in Table S1 (Supporting Information). The nucleoprotein extraction kit was from Shanghai Sangon Biotechnology Co. Ltd. (Shanghai, China). Reagents for polyacrylamide gel electrophoresis, including 40% acrylamide mix solution, ammonium persulfate (APS), 1,2-bis-(dimethylamino)ethane (TEMED), ethidium bromide (EB), and protein markers, were also purchased from Shanghai Sangon Biotechnology Co. Ltd. (Shanghai, China). All other chemicals involved in this work were analytical-grade. All aqueous solutions were freshly prepared in ultrapure water (≥18MΩ, Milli-Q, Millipore).

Apparatus and Characterization. UV−vis spectra were recorded on a UV-3600 spectrophotometer (Shimadzu, Kyoto, Japan), and fluorescence measurements were carried out on a RF-5301PC (Shimadzu, Kyoto, Japan). The excitation/emission wavelengths were set at 585 nm/635 nm. The fluorescence lifetime test was carried out on fluorescence spectroscopy instrumentation (FM-4P-TCSPC, Horiba Jobin Yvon). Circular dichroism (CD) spectra were obtained on a J-810 spectropolarimeter, and nuclear staining study was conducted with a confocal microscope (TCS SP5, Leica, Germany). Fluorescence gel imaging was carried out with a Bio-Rad imaging system (serial no. 76S/06725). T_m values and the secondary structure of DNA oligos were analyzed by OligoAnalyzer 3.1 (free online software from IDT).

Synthesis of Fluorescent Silver Nanoclusters. DNA-stabilized Ag NCs were synthesized according to the procedure described elsewhere with slight modifications.[32,43,44] Briefly, 6 μL of 250 μM NC-AS1411-T5 was mixed with 4.7 μL of 20 mM phosphate (pH 7.0) buffer, and then 3.2 μL of 10 mM $AgNO_3$ solution was added to reach a nucleobase to Ag^+ molar ratio of 2:1. After being chilled on ice for 15 min, the mixture was reduced by quickly adding 16.1 μL of 2 mM $NaBH_4$, followed by vigorous shaking for 1 min. The reaction was kept at 4 °C for at least 5 h before use, based on their fluorescence evolution with time (Figure S1 in Supporting Information). Ag NCs stabilized with other DNA sequences listed in Table S1 in Supporting Information were synthesized by the same procedure while the amounts of $AgNO_3$ and $NaBH_4$ were adjusted to satisfy the base to Ag^+ ratio of 2:1.

Circular Dichroism Measurement. In order to confirm the G-quadruplex structure of AS1411 after the modification with poly(cytosine), the CD spectra of AS1411 and NC-AS1411-T5 in the presence of 0.1 M NaCl were analyzed on a J-810 spectropolarimeter. The CD spectra were recorded from 220 to 500 nm and the corresponding parameter settings were as follows: scanning speed 50 nm/min, response time 0.25 s, bandwidth 1.0 nm, and 2 times accumulation.[45] The concentrations of DNA samples were 12 μM.

Polyacrylamide Gel Electrophoresis Analysis. Polyacrylamide gel (4%) was employed to examine the binding of NC-AS1411-T5 to nucleolin. Nuclear proteins were extracted from MCF-7 cells by use of a nucleoprotein extraction kit. Nuclear extracts were then incubated with FAM-AS1411 or FAM-NC-AS1411-T5 at 37 °C for 1 h. At last, the complexes were resolved by gel electrophoresis on 4% polyacrylamide at

dx.doi.org/10.1021/ac3003402 | Anal. Chem. 2012, 84, 4140−4146

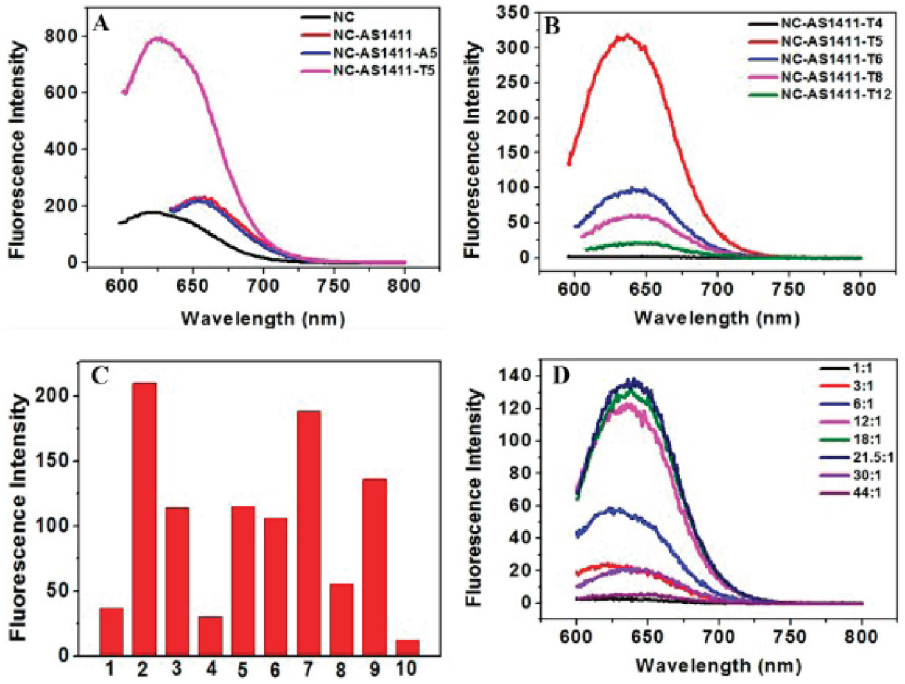

Figure 1. (A) Fluorescence emission spectra of Ag NCs templated by NC, NC-AS1411, NC-AS1411-A5, or NC-AS1411-T5. (B) Effect of linker length on the fluorescence emission of Ag NCs. (C) Buffer optimization. (1) 40 mM ammonium acetate; (2) 20 mM ammonium acetate; (3) 80 mM ammonium acetate; (4) 10 mM citrate buffer; (5) 20 mM citrate buffer; (6) 5 mM PBS buffer; (7) 20 mM PBS buffer; (8) 5 mM acetate/acetic; (9) 10 mM Tris-HCl; (10) 10 mM Tris-HAc. (D) Effect of oligonucleotide:Ag^+ ratio.

100 V for 75 min and recorded by the fluorescence imaging system.

Cell Culture. MCF-7 human breast cancer cell line and NIH-3T3 mouse fibroblast cell line were obtained from Nanjing KeyGen Biotech Co. Ltd. (Nanjing, China). MCF-10A human normal mammary epithelial cells were obtained from Shanghai Bioleaf Biotech Co. Ltd. (Shanghai, China). MCF-7 cells were seeded in LDMEM medium (Gibco, Grand Island, NY) supplemented with 10% fetal calf serum (FCS, Sigma), penicillin (100 μg/mL), and streptomycin (100 μg/mL) in 5% CO_2, 37 °C incubator. NIH-3T3 mouse fibroblast cells and MCF-10A cells were cultured similarly except that LDMEM was replaced by HDMEM. The cells were harvested from 90% confluent cell culture plates and the cell density was determined by use of a Petroff-Hausser cell counter prior to experiments.

Confocal Laser Microscopy Assay. MCF-7 cells (1×10^5) were seeded onto 12-mm sterile coverslips in a 24-well plate. After 24 h, cells were incubated with NC-AS1411-T5-stabilized Ag NCs for 30 min at 4 °C after being washed three times with phosphate-buffered saline (PBS). To remove the unbound Ag NCs, the cells were washed three times with PBS. Then cells were fixed for 20 min in 200 μL of 3.7% paraformaldehyde. After the fixation, cells were washed three times with PBS, followed by nucleus staining with 4′,6-diamidino-2-phenylindole dihydrochloride (DAPI). Ten minutes later, the cells were further washed three times with PBS buffer. The side of coverslip with fixed cells was topped by a glass slide with 10 μL drop of 50% glycerol/PBS (v/v). Then the glass slide was inverted and placed above a 20× objective on the confocal microscope. The Ag NCs were excited with 543 nm and DAPI with UV. NIH-3T3 mouse fibroblast cells and MCF-10A cells were treated with the same procedure as control.

***Z*-Axis Scanning.** In order to examine whether Ag NCs were internalized into the nucleus, *Z*-axis scanning was introduced. Parameters involved in the *Z*-axis scanning included the beginning and ending *Z*-value for the sample, thickness of the sample, and number of optical sections within the volume. Micrographs were taken while the focal plane was moved in incremental steps from the bottom of the cells up to the coverslip.

MTT Assay. Cells (1×10^4) were seeded in each well of a 96-well plate before exposure to AS1411, NC-AS1411-T5, Ag NCs, or Ag^+ of various concentrations for 48 h. Prior to the exposure, synthesized Ag NCs were centrifuged for 100 min at 10 000 rpm through a 3 kDa cutoff filter to remove unbound Ag^+ from the NC-AS1411-T5-templated Ag NCs. Medium was removed after exposure. Cells were washed twice with PBS buffer before the addition of DMEM containing MTT (5 mg/mL) and further incubated at 5% CO_2, 37 °C for another 4 h. Then the medium containing MTT was replaced by 100 μL of dimethyl sulfoxide (DMSO) to solubilize the formazan crystals precipitate. The plate was shaken for 15 min at 37 °C before the measurement of optical absorbance at 492 nm on a model 680 microplate reader (Bio-Rad).[46]

RESULTS AND DISCUSSION

Preparation of Aptamer-Functonalized Ag NCs. Silver nanoclusters are generally produced by the reduction of a mixture of DNA scaffold and silver nitrate by sodium borohydride. The distinct spectrum of specific clusters, covering from blue-green to near-infrared, is highly dependent on the sequence of DNA scaffold.[25] It was reported that bright and near-IR-emitting Ag NCs could be generated through ssDNA consisting of 12 cytosines.[16] Thus we first added 12 cytosines at the 5′ end of AS1411 (termed NC-AS1411 in Table S1 in Supporting Information) to synthesize Ag NCs.

dx.doi.org/10.1021/ac3003402 | *Anal. Chem.* 2012, 84, 4140−4146

The fluorescence intensity of Ag NCs on modified template was slightly stronger than those produced by pure C12 template (Figure 1A). Considering the steric hindrance between aptamer and synthesized Ag NCs, a linker (AAAAA or TTTTT) was incorporated between AS1411 and cytosine-rich sequence. As shown in Figure 1A, the fluorescence intensity of Ag NCs with -TTTTT- linker was about 6-fold than those with -AAAAA- linker. It should be mentioned that Ag NCs with -AAAAA- linker featured even lower fluorescence intensity than those without a linker. The reason might be that the attachment of Ag to -TTTTT- loop cannot be excited by visible light, while Ag in -AAAAA- loop has weak fluorescence emission at 534.9 ± 2.8 nm, which might interfere with the formation of C12-templated Ag NCs.[47] -TTTTT- linker was chosen for the following experiment. Additionally, the effect of linker length was also investigated (the sequences are listed in Table S1 in Supporting Information) and NC-AS1411-T5 showed the strongest fluorescence emission (Figure 1B). Other parameters were also optimized to produce Ag NCs with good fluorescence properties. Ten different buffers commonly used were compared in the synthesis of Ag NCs. As shown in Figure 1C, 20 mM ammonium acetate (pH 7.0) presented the highest fluorescence signal and 20 mM PBS (pH 7.0) was slightly weaker; however, 20 mM PBS was selected due to its better biological compatibility. For a certain sequence, ratio of nucleotides to Ag^+ was crucial in the process of generating fluorophore.[48] Here the ratio of oligonucleotide to Ag^+ was varied from 1:1 to 44:1, and the best result came from 21.5:1, that is, 2:1 for nucleobase:Ag^+ (Figure 1D). This result was consistent with the phenomenon that the optimal nucleobase:Ag^+ ratio for maximum fluorescence emission was approximately two bases per silver.[18,21,44]

Characterization of NC-AS1411-T5-Stabilized Ag NCs. The NC-AS1411-T5-stabilized Ag NCs showed fluorescence emission at 635 nm when excited at 585 nm (Figure 2A), and the fluorescence lifetime was 1.85 ± 0.086 ns (Figure 2B). Two peaks of UV absorption at 440 and 567 nm were consistent with nanoclusters and NC-AS1411-T5-templated Ag NCs, respectively.[49] Transmission electron microscopy (TEM) image in Figure 2C revealed that the Ag NCs were monodispersed and the average size in the distribution of Ag NCs was 1.5 nm. The high-resolution (HRTEM) image of an individual Ag NC demonstrated the good crystallinity of the obtained Ag NCs (Figure 2D). We also calculated the quantum yield of the Ag NCs. with rhodamine 101 inner salt in ethanol as the reference standard. at room temperature to be 40.1%, which was better than what had been reported.

To confirm the secondary structure of AS1411 with the addition of poly(cytosine) sequence, the circular dichroism experiment was performed. Figure S2A (Supporting Information) shows the CD spectra of AS1411 and NC-AS1411-T5 in the presence of 0.1 M NaCl. It is known that "folded" quadruplexes have a CD spectrum characterized by a positive ellipticity maximum at 295 nm and a negative minimum at 265 nm, while the "parallel" type have a positive maximum at 264 nm and a negative minimum at 240 nm.[50] With poly(cytosine), the secondary structure of AS1411 switched from a "parallel" type to a "folded" type. We further tested the binding affinity of such "folded" quadruplexes to nucleolin by 4% native polyacrylamide gel. The nuclear protein extracts were incubated with FAM-AS1411 or FAM-NC-AS1411-T5 at 37 °C for 1 h before loading. The result (Figure S2B, Supporting Information) indicated that NC-AS1411-T5 retained its binding affinity

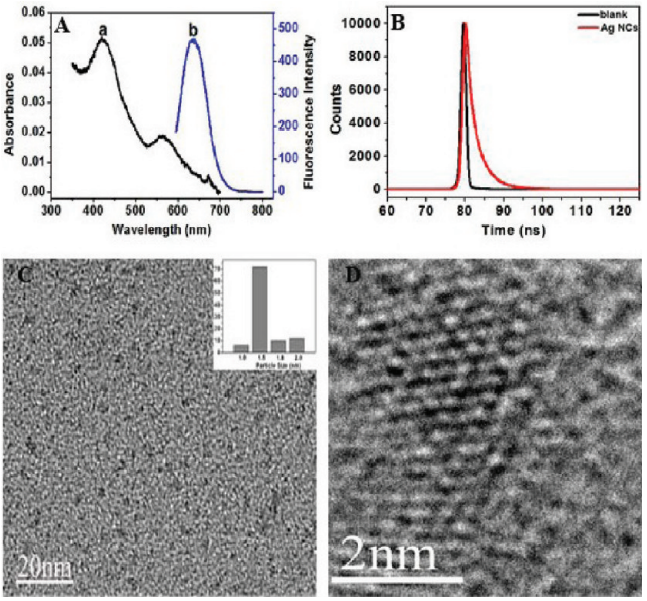

Figure 2. (A) (a) UV absorption spectra and (b) fluorescence emission spectra of NC-AS1411-T5-templated Ag NCs. (B) Fluorescence lifetime of NC-AS1411-T5-stabilized Ag NCs dispersed in PBS. Excitation wavelength: 585 nm. (C) TEM image of Ag NCs. (Inset) Distribution of particle size. (D) HRTEM image of an individual Ag NC.

to nucleolins, which provided their potential application in the following nuclear staining.

Nuclear Staining by NC-AS1411-T5-Stabilized Ag NCs. Brightness of a fluorescence probe is crucial for obtaining high-resolution images.[51] Good quantum yield of the Ag NCs is beneficial to cellular staining and imaging. Due to the binding affinity being retained in AS1411-poly(cytosine), we wanted to test if the NC-AS1411-T5-stabilized Ag NCs could be used as the specific fluorescent probe for cell imaging. As illustrated in Figure 3, NC-AS1411-T5-templated Ag NCs were internalized into MCF-7 cells easily (A) while internalization was not observed in NIH-3T3 mouse fibroblast cells (B) and MCF-10A human normal mammary epithelial cells (C), indicating such internalization of Ag NCs was cell-specific. By comparing phase-contrast image with nuclear DAPI staining, we found the intracellular Ag NCs were mainly accumulated in nuclei and less in the cytoplasm of MCF-7 cells (Figure 4).

Three-dimensional images of entire cells stained by Ag NCs were further obtained. MCF-7 cells stained by NC-AS1411-T5-stabilized Ag NCs were imaged at different depths along the *Z*-axis. Micrographs were taken while the focal plane was moved in incremental depths from the bottom of cells up to the coverslip. A typical section image (Figure 5) demonstrated that part of the NC-AS1411-T5-stabilized Ag NCs were present in the cell nuclear fraction.[52] Since nucleolin is expressed at high levels in malignant cells and it is a carrier protein that can transfer molecules between the cell surface and the nucleus, one possible mechanism for the internalization of NC-AS1411-T5-stabilized Ag NCs is via nucleolin-mediated endocytosis.[53−55]

MTT Assay. AS1411 is currently under phase II clinical trials as an anticancer reagent. In order to confirm the therapeutically effective dose of NC-AS1411-T5-templated Ag NCs to inhibit cancer cell proliferation, the MTT assay experiment was performed, which revealed that growth of MCF-7 cells was significantly hindered after exposure to AS1411, NC-AS1411-

dx.doi.org/10.1021/ac3003402 | *Anal. Chem.* 2012, 84, 4140−4146

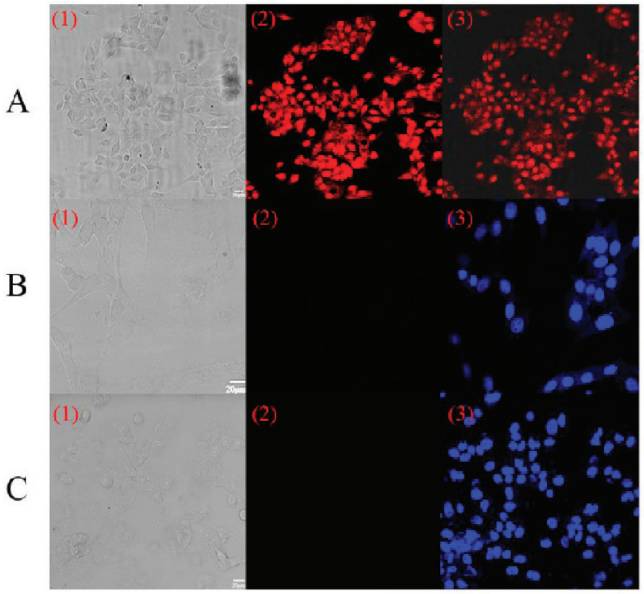

Figure 3. Confocal laser scanning microscopy of (A) MCF-7 human breast cancer cells, (B) NIH-3T3 mouse fibroblast cells, and (C) MCF-10A human normal mammary epithelial cells incubated with NC-AS1411-T5-stabilized Ag NCs at 4 °C for 30 min: (1) bright-field images; (2) Ag NCs fluorescence images (red); (A3) overlap of corresponding fluorescence image and bright-field image; (B3, C3) fluorescence images with DAPI nuclear staining (blue). The Ag NCs were excited with 543 nm and DAPI with UV. Scale bar, 20 μm. Under the same procedure, there were no detectable emissions from the control cells.

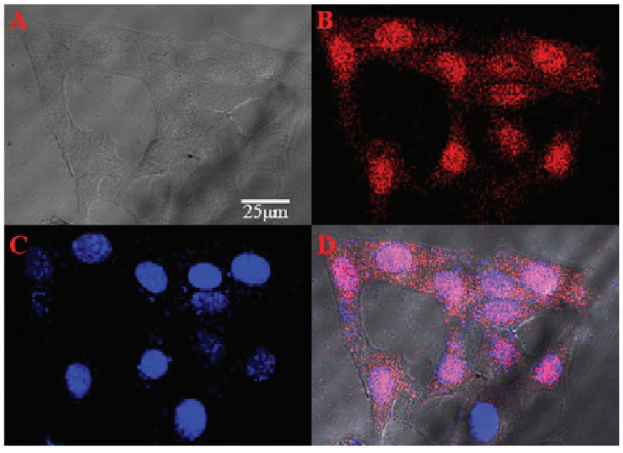

Figure 4. Intracellular distribution of internalized NC-AS1411-T5-stabilized Ag NCs. MCF-7 cells were incubated with Ag NCs at 4 °C for 30 min. After being fixed with paraformaldehyde for 20 min, the cells were nuclear-staining with DAPI for 10 min. The fluorescence imaging was then recorded by confocal laser microscopy. (A) Bright-field images; (B) fluorescence images of Ag NCs (red); (C) fluorescence images with DAPI nuclear staining (blue); (D) overlap of corresponding fluorescence image and bright-field image. Scale bar, 25 μm.

T5, or NC-AS1411-T5-templated Ag NCs (Figure 6). The Ag NCs displayed a greater inhibition effect than AS1411 and NC-AS1411-T5. It was reported that NP-AS1411 could block the pathways for the translocation of transcription factors to the nucleus to activate antiapoptotic genes more effectively than pure AS1411.[56] Here, it might be the same mechanism by

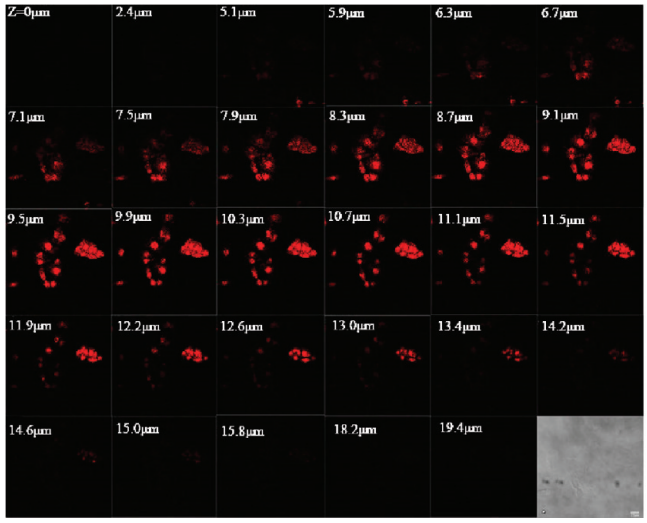

Figure 5. *Z*-Axis scanning image of internalized NC-AS1411-T5-stabilized Ag NCs recorded by confocal microscope. Micrographs were taken while the focal plane was moved in incremental steps from the bottom of the cell up to the coverslip. Scale bar, 25 μm.

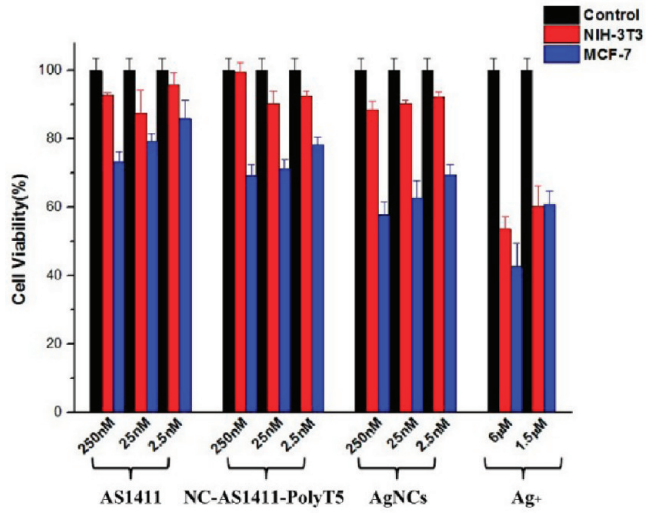

Figure 6. MCF-7 human breast cancer cell viability and NIH-3T3 mouse fibroblast cell viability after 48 h exposure to AS1411, NC-AS1411-T5, NC-AS1411-T5-templated Ag NCs or $AgNO_3$ of various concentrations. $AgNO_3$ at 6 μM is equivalent to the dosage used for the synthesis of 250nM Ag NCs .

which NC-AS1411-T5-stabilized Ag NCs enhanced the inhibition—accumulation of AgNCs in nuclei. Exposure of AS1411, NC-AS1411-T5, or Ag NCs to NIH-3T3 mouse fibroblast cells did not have any obvious cytotoxic effect in control experiments, indicating the cytocompatibility of NC-AS1411-T5-stabilized Ag NCs. It should be noticed that Ag^+ exhibited significant toxicity to both cell lines with the same dosage as in the synthesis of Ag NCs as shown in Figure 6, which confirmed the antiproliferation effect resulted from the NC-AS1411-T5-templated Ag NCs and not Ag^+.

General Design for Other Aptamer-Functionalized Ag NCs. The integration of signal reporter and molecular recognition is the basis for target detection and biological labeling and imaging.[57−59] The in situ synthesis for fluorescent Ag NCs containing aptamer is a simple and cost-friendly one-step process without additional conjugation of biorecognition

dx.doi.org/10.1021/ac3003402 | *Anal. Chem.* 2012, 84, 4140−4146

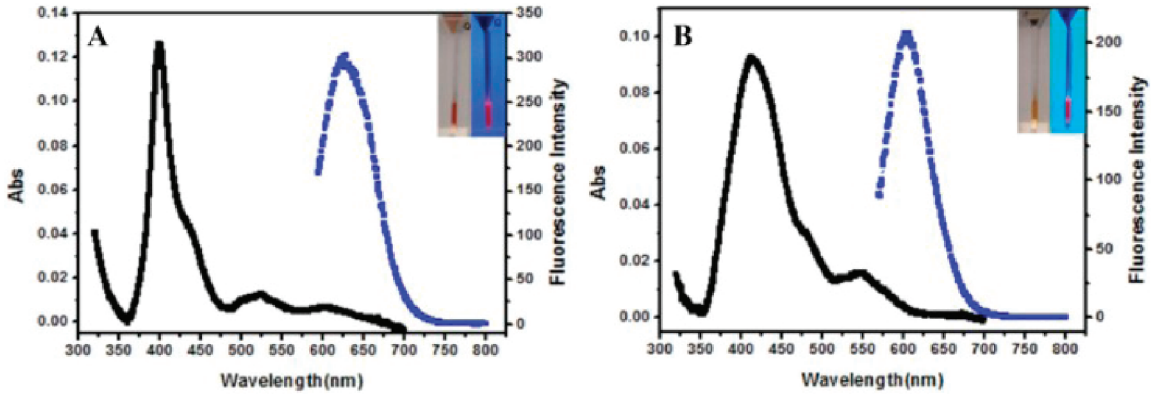

Figure 7. UV absorption spectra (black) and fluorescence emission spectra (blue) of (A) NC-MUC1-stabilized Ag NCs and (B) NC-Sgc8c-stabilized Ag NCs. (Insets) Photographs of Ag NCs solution under ambient light (left) and illuminated by a UV lamp of 365 nm (right).

molecules to fluorophores.[60] However, the synthesis of aptamer-functionalized Ag NCs with decent fluorescence properties is essential for their applications in biological imaging. It is known that the spectrum of DNA-templated Ag NCs is dependent on the oligo sequence and the secondary structure of DNA strands bearing silver atoms.[47] Herein, we hypothesized the T5 loop is crucial to the fluorescence of Ag NCs, on the basis of the above data and further study of the secondary structure of NC-AS1411-T5 (shown in Figure S3 in Supporting Information). As shown in Figure S4 (Supporting Information), without such T5 loop, the emission was much weaker than those with T5 loop. To substantiate our hypothesis, another two aptamers, Sgc8c and MUC1, were linked with poly(cytosine) via a T5 loop to synthesize Ag NCs. Sgc8c is an aptamer selected through cell-SELEX to recognize T-cells,[40,61] and MUC1 aptamer can specifically bind MUC1 protein on the surface of tumor cells with high affinity.[62−64] UV and fluorescence spectra shown in Figure 7 confirmed these Ag NCs provided good emission intensity. Their quantum yields were calculated to be 25.2% (MUC1 aptamer) and 48.0% (Sgc8c) with rhodamine 101 inner salt as the reference standard. The difference might stem from the different microenvironment in each aptamer.[65]

CONCLUSIONS

In this study, we integrated AS1411 with poly(cytosine) via a -TTTTT- loop and used it as the scaffold to synthesize Ag NCs through a one-step process. The fluorescence quantum yield of the obtained Ag NCs could reach 40.1% with rhodamine101 inner salt as the reference standard. The binding affinity of NC-AS1411-T5-templated Ag NCs to nucleolin provided opportunities for their application in intracellular imaging and nuclear staining. Furthermore, Ag NCs stabilized by NC-Sgc8c and NC-MUC1 with good fluorescence emission properties indicated the universality of scaffold design and would undoubtedly broaden the applications of functionalized Ag NCs in biological areas.

ASSOCIATED CONTENT

Supporting Information

One table, listing names and sequences of oligonucleotides, and six figures, showing fluorescence evolution of NC-AS1411-T5-templated Ag NCs with time; CD spectra of AS1411 and NC-AS1411-T5 and gel shift analysis of FAM-AS1411 and FAM-NC-AS1411-T5 binding to nucleolin; secondary structure and T_m determinations; fluorescence emission spectra of Ag NCs templated by NC, NC-AS1411, AS1411, NC-AS1411-T5, and NC-T5; stability of NC-AS1411-T5-templated Ag NCs; and absorbance and fluorescence emission spectra of rhodamine 101 and NC-AS1411-T5-stabilized Ag NCs. This material is available free of charge via the Internet at http://pubs.acs.org.

AUTHOR INFORMATION

Corresponding Author

*Tel/fax: +86 25 83597204. E-mail: jjzhu@nju.edu.cn (J.-J.Z.) or Jiangliping@nju.edu.cn (L.-P.J.).

Notes

The authors declare no competing financial interest.

ACKNOWLEDGMENTS

This work was supported by the National Natural Science Foundation of China (Grants 50972058, 21020102038, and 21121091). We also appreciate the support from Doctoral Foundation from Ministry of Education (20100091110023) and National Basic Research Program of China (2011CB933502).

REFERENCES

(1) Hoffman, R. M. *Nat. Rev. Cancer* **2005**, *5*, 796−806.
(2) Misgeld, T.; Kerschensteiner, M. *Nat. Rev. Neurosci.* **2006**, *7*, 449−463.
(3) Zernicka-Goetz, M. *Nat. Rev. Mol. Cell Biol.* **2005**, *6*, 919−928.
(4) Gao, X.; Cui, Y.; Levenson, R. M.; Chung, L. W. K.; Nie, S. *Nat. Biotechnol.* **2004**, *22*, 969−976.
(5) Bagalkot, V.; Zhang, L. F.; Levy-Nissenbaum, E.; Jon, S.; Kantoff, P. W.; Langer, R.; Farokhzad, O. C. *Nano Lett.* **2007**, *7* (10), 3065−3079.
(6) Hoyer, P.; Staudt, T.; Engelhardt, J.; Hell, S. W. *Nano Lett.* **2011**, *11* (1), 245−250.
(7) Tada, H.; Higuchi, H.; Wanatabe, T. M.; Ohuchi, N. *Cancer Res.* **2007**, *67*, 1138−1144.
(8) Hong, H.; Shi, J.; Yang, Y. N.; Zhang, Y.; Engle, J. W.; Nickles, R. J.; Wang, X. D.; Cai, W. B. *Nano Lett.* **2011**, *11*, 3744−3750.
(9) Jaiswal, J. K.; Mattoussi, H.; Mauro, J. M.; Simon, S. M. *Nat. Biotechnol.* **2003**, *21*, 47−51.
(10) Michalet, X.; Pinaud, F. F.; Bentolila, L. A.; Tsay, J. M.; Doose, S.; Li, J. J.; Sundaresan, G.; Wu, A. M.; Gambhir, S. S.; Weiss, S. *Science* **2005**, *307*, 538−543.
(11) Kuno, M.; Fromm, D. P.; Hamann, H. F.; Gallagher, A.; Nesbitt, D. J. *J. Phys. Chem.* **2000**, *112*, 3117−3120.
(12) Derfus, A. M.; Chan, W. C. W.; Bhatia, S. N. *Nano Lett.* **2004**, *4*, 11−18.
(13) Lee, S. F.; Osborne, M. A. *J. Am. Chem. Soc.* **2007**, *129*, 8936−8937.

(14) Wang, H. H.; Lin, C. A. J.; Lee, C. H.; Lin, Y. C.; Tseng, Y. M.; Hsieh, C. L.; Chen, C. H.; Tsai, C. H.; Hsieh, C. T.; Shen, J. L.; Chan, W. H.; Chang, W. H.; Yeh, H. I. *ACS Nano* **2011**, *5* (6), 4337−4344.
(15) Wang, Y. L.; Chen, J. J.; Irudayaraj, J. *ACS Nano* **2011**, *5* (12), 9718−9725.
(16) Vosch, T.; Antoku, Y.; Hsiang, J. C.; Richards, C. I.; Gonzalez, J. I.; Dickson, R. M. *Proc. Natl. Acad. Sci. U.S.A.* **2007**, *104*, 12616−12621.
(17) de Souza, N. *Nat. Methods* **2007**, *4*, 540−540.
(18) Richards, C. I.; Choi, S.; Hsiang, J. C.; Antoku, Y. *J. Am. Chem. Soc.* **2008**, *130*, 5038−5039.
(19) Gwinn, E. G.; O'Neill, P.; Guerrero, A. J.; Bouwmeester, D.; Fygenson, D. K. *Adv. Mater.* **2008**, *20*, 279−283.
(20) Sharma, J.; Yeh, H. C.; Yoo, H.; Werner, J. H.; Martinez, J. S. *Chem. Commun.* **2010**, *46*, 3280−3282.
(21) Guo, W. W.; Yuan, J. P.; Dong, Q. Z.; Wang, E. K. *J. Am. Chem. Soc.* **2010**, *132*, 932−934.
(22) Su, Y. T.; Lan, G. Y.; Chen, W. Y.; Chang, H. T. *Anal. Chem.* **2010**, *82*, 8566−8572.
(23) Han, B. Y.; Wang, E. K. *Biosens. Bioelectron.* **2011**, *26*, 2585−2589.
(24) Yang, S. W.; Vosch, T. *Anal. Chem.* **2011**, *83*, 6935−6939.
(25) Petty, J. T.; Sengupta, B.; Story, S. P.; Degtyareva, N. N. *Anal. Chem.* **2011**, *83*, 5957−5964.
(26) Petty, J. T.; Story, S. P.; Juarez, S.; Votto, S. S.; Herbst, A. G.; Degtyareva, N. N.; Sengupta, B. *Anal. Chem.* **2012**, *84* (1), 356−364.
(27) Huang, Z. Z.; Pu, F.; Lin, Y. H.; Ren, J. S.; Qu, X. G. *Chem. Commun.* **2011**, *47*, 3487−3489.
(28) Guo, W. W.; Yuan, J. P.; Wang, E. K. *Chem. Commun.* **2009**, *23*, 3395−3397.
(29) Lan, G. Y.; Huang, C. C.; Chang, H. T. *Chem. Commun.* **2010**, *46*, 1257−1259.
(30) Yu, J. H.; Choi, S.; Richards, C. I.; Antoku, Y.; Dickson, R. M. *Photochem. Photobiol.* **2008**, *84* (6), 1435−1439.
(31) Díez, I.; Robin, H. A. R. *Springer Ser. Fluoresc.* **2010**, *9*, 307−332.
(32) Yu, J. H.; Choi, S.; Dickson, R. M. *Angew. Chem., Int. Ed.* **2009**, *48*, 318−320.
(33) Sun, Z. P.; Wang, Y. L.; Wei, Y. T.; Liu, R.; Zhu, H. R.; Cui, Y. Y.; Zhao, Y. L.; Gao, X. Y. *Chem. Commun.* **2011**, *47*, 11960−11962.
(34) Ponomarev, V. *Cancer Cell Ther.* **2009**, *50* (7), 1013−1016.
(35) Yu, J. H.; Patel, S. A.; Dickson, R. M. *Angew. Chem., Int. Ed.* **2007**, *46*, 2028−2030.
(36) Bates, P. J.; Laber, D. A.; Miller, D. M.; Thomas, S. D.; Trent, J. O. *Exp. Mol. Pathol.* **2009**, *86*, 151−164.
(37) Mi, Y. C.; Thomas, S. D.; Xu, X. H.; Casson, L. K.; Miller, D. M.; Bates, P. J. *J. Biol. Chem.* **2003**, *278* (10), 8572−8579.
(38) Giljohann, D. A.; Seferos, D. S.; Patel, P. C.; Millstone, J. E.; Rosi, N. L.; Mirkin, C. A. *Nano Lett.* **2007**, *7* (12), 3818−3821.
(39) Antoku, Y.; Hotta, J. I.; Mizuno, H.; Dickson, R. M.; Hofkens, J.; Vosch, T. *Photochem. Photobiol. Sci.* **2010**, *9*, 716−721.
(40) Shangguan, D. H.; Cao, Z. C.; Chen, H. W.; Mallikaratchy, P.; Sefah, K.; Yang, C. J.; Tan, W. H. *Proc. Natl. Acad. Sci. U.S.A.* **2006**, *103*, 11838−11843.
(41) Xiao, Z. Y.; Shangguan, D. H.; Cao, Z. H.; Fang, X. H.; Tan, W. H. *Chem.—Eur. J.* **2008**, *14*, 1769−1775.
(42) Ferreira, C. S. M.; Papamichael, K.; Guibault, G.; Schwarzacher, T.; Gariepy, J.; Missailidis, S. *Anal. Bioanal. Chem.* **2008**, *390*, 1039−1050.
(43) Lan, G. Y.; Huang, C. C.; Chang, H. T. *Chem. Commun.* **2010**, *46*, 1257−1259.
(44) Petty, J. T.; Zhang, J.; Hud, N. V.; Dickson, R. M. *J. Am. Chem. Soc.* **2004**, *126*, 5207−5212.
(45) Shieh, Y. A.; Yang, S. J.; Wei, M. F.; Shieh, M. J. *ACS Nano* **2010**, *4* (3), 1433−1442.
(46) Guo, J. W.; Gao, X. L.; Su, L. N.; Xia, H. M.; Cu, G. Z.; Pang, Z. Q.; Jiang, X. G.; Yao, L.; Chen, J.; Chen, H. Z. *Biomaterials* **2011**, *32*, 8010−8020.
(47) Gwimn, E. G.; O'Neill, P.; Guerrero, A. J.; Bouwmeester, D.; Fygenson, D. K. *Adv. Mater.* **2008**, *20*, 279−283.
(48) Choi, S.; Yu, J. H.; Patel, S. A.; Tzeng, Y. L.; Dickson, R. M. *Photochem. Photobiol. Sci.* **2011**, *10*, 109−115.
(49) Ritchie, C. M.; Johnsen, K. R.; Kiser, J. R.; Antoku, Y.; Dickson, R. M.; Petty, J. T. *J. Phys. Chem. C* **2007**, *111*, 175−181.
(50) Dapic, V.; Abdomerovic, V.; Marrington, R.; Peberdy, J.; Rodger, A.; Trent, J. O.; Bates, P. J. *Nucleic Acids Res.* **2003**, *31* (8), 2097−2107.
(51) Tanaka, S. I.; Miyazaki, J.; Tiwari, D. K.; Jin, T.; Inouye, Y. *Angew. Chem.* **2011**, *123*, 451−455.
(52) Li, W.; Yang, X. H.; Wang, K. M.; Tan, W. H.; He, Y.; Guo, Q. P.; Tang, H. X.; Liu, J. B. *Anal. Chem.* **2008**, *80*, 5002−5008.
(53) Mi, Y. C.; Thomas, S. D.; Xu, X. H.; Casson, L. K.; Miller, D. M.; Bates, P. J. *J. Biol. Chem.* **2003**, *278* (10), 8572−8579.
(54) Sald, E. A.; Krust, B.; Nlsole, S.; Svab, J.; Brland, J. P.; Hovanessian, A. G. *J. Biol. Chem.* **2002**, *277*, 37492−37502.
(55) Ko, M. H.; Kim, S.; Kang, W. J.; Lee, J. H.; Kang, H.; Moon, S. H.; Hwang, D. W.; Ko, H. Y.; Lee, D. S. *Small* **2009**, *5* (10), 1207−1212.
(56) Choi, J. H.; Chen, K. H.; Han, J. H.; Chaffee, A. M.; Strano, M. S. *Small* **2009**, *5* (6), 672−675.
(57) Tainaka, K.; Sakaguchi, R.; Hayashi, H.; Nakano, S.; Liew, F. F.; Morii, T. *Sensors* **2010**, *10*, 1355−1376.
(58) Zhou, X. M.; Tang, Y. H.; Xing, D. *Anal. Chem.* **2011**, *83*, 2906−2912.
(59) Juskowiak, B. *Anal. Bioanal. Chem.* **2011**, *399* (9), 3157−3176.
(60) Yin, J. J.; He, X. X.; Wang, K. M.; Qing, Z. H.; Wu, X.; Shi, H.; Yang, X. H. *Nanoscale* **2012**, *4*, 110−112.
(61) Xiao, Z. Y.; Shangguan, D. H.; Cao, Z. H.; Fang, X. H.; Tan, W. H. *Chem.—Eur. J.* **2008**, *14*, 1769−1775.
(62) Ferreira, C. S. M.; Matthews, C. S.; Missailidis, S. *Tumor Biol* **2006**, *27*, 289−301.
(63) von Mensdorff-Pouilly, S; Snijdewint, F. G. M.; Verstraeten, A. A.; Verheijen, R. H.; Kenemans, P. *Int. J. Biol. Markers* **2000**, *15*, 343−56.
(64) Gendler, S. J. *J. Mammary Gland Biol. Neoplasia* **2001**, *6*, 339−53.
(65) Schultz, D.; Gwinn, E. *Chem. Commun.* **2011**, *47*, 4715−4717.